Orthovanadate and orthophosphate inhibit muscle force via two different pathways of the myosin ATPase cycle

Orthovanadate and Orthophosphate Inhibit Muscle Force via Two Different Pathways of the Myosin ATPase Cycle

Marco Caremani,[†] Steve Lehman,[‡] Vincenzo Lombardi,[†] and Marco Linari[†*]
[†]Laboratory of Physiology, Department of Evolutionary Biology, Università di Firenze, Florence, Italy; and [‡]Department of Integrative Biology, University of California, Berkeley, California

ABSTRACT Measurements of the half-sarcomere stiffness during activation of skinned fibers from rabbit psoas (sarcomere length 2.5 μm, temperature 12°C) indicate that addition of 0.1 mM orthovanadate (Vi) to the solution produces a drop to ~1/2 in number of force-generating myosin motors, proportional to the drop in steady isometric force (T_0), an effect similar to that produced by the addition of 10 mM phosphate (Pi). However, in contrast to Pi, Vi does not change the rate of isometric force development. The depression of T_0 in a series of activations in presence of Vi is consistent with an apparent second-order rate constant of ~1 $\times$ 10^3 M^{-1} s^{-1}. The rate constant of T_0 recovery in a series of activations after removal of Vi is 3.5 $\times$ 10^{-2} s^{-1}. These results, together with the finding in the literature that the ATPase rate is reduced by Vi in proportion to isometric force, are reproduced with a kinetic model of the acto-myosin cross-bridge cycle where binding of Vi to the force-generating acto-myosin-ADP state induces detachment from actin to form a stable myosin-ADP-Vi complex that is not able to complete the hydrolysis cycle and reenters the cycle only via reattachment to actin upon activation in Vi-free solution.

INTRODUCTION

Force and shortening in striated muscle are generated by myosin II molecular motors working in arrays in the half-sarcomere. The myosin head (M) cyclically attaches to an actin site (A) on the thin filament and undergoes a working stroke associated with the release of the hydrolysis product orthophosphate (Pi). In Ca^{2+}-activated skinned muscle fibers, it has been recently demonstrated that addition of Pi decreases the force developed during isometric contraction (T_0) in proportion to the number of myosin motors attached to actin in each half-thick filament (1).

This has important consequences, because it addresses longstanding questions about the chemo-mechanical coupling of the acto-myosin ATPase reaction in situ: the finding that the increase of [Pi] inhibits the rate of the ATP hydrolysis in isometric contraction much less than isometric force (2–8) can be explained if strongly bound force-generating myosin motors detach from actin at an early stage of the ATPase cycle, with Pi still bound to its catalytic site and then rapidly release the hydrolysis products to bind another ATP (9). Thus, the conventional reaction pathway for the myosin-actin ATPase cycle must be integrated with a branch in the cycle according to Scheme 1, as follows:

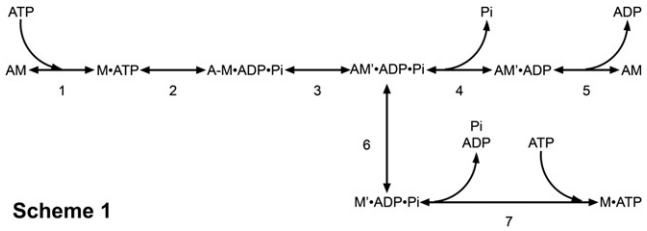

Scheme 1

According to this scheme, in isometric conditions, ATP binds to the actomyosin (AM) complex (step 1), promotes the rapid dissociation of myosin from actin (incorporated in step 1), and then hydrolizes ATP (step 2). The myosin with the ATP hydrolysis products (ADP and Pi) is in rapid equilibrium with the weakly bound AM.ADP.Pi state. Myosin, with ADP and Pi bound, attaches to actin forming a strong bound cross-bridge and generates force (step 3). This step sets the fraction of attached myosin motors to ~0.3 (10). Pi is released in a rapid reaction (step 4 (11)), leading to the AM′.ADP state.

The subsequent ADP release step (step 5) occurs at a low rate (12–14). The branched pathway (9) implies that myosin in the AM′.ADP.Pi force-generating state can detach before release of Pi and ADP (step 6), generating a M′.ADP.Pi state that rapidly releases Pi and ADP and binds a new ATP (step 7) to enter a new cycle. The flux through this pathway increases with the increase in Pi concentration, providing the alternative pathway for maintaining high the ATPase rate, notwithstanding the reduced number of strongly bound force-generating motors.

Orthovanadate (Vi) is a phosphate analog that in solution binds to myosin and inhibits its ATPase, forming a stable inactive M.ADP.Vi complex (rate constant of ADP and Vi dissociation ~10^{-5} s^{-1}) (15). Actin binding to this complex increases Vi and ADP release ~10^5 times (16). In permeabilized muscle fibers, Vi suppresses isometric tension (17,18), half-sarcomere stiffness (19,20), and ATPase rate (21). The drop in isometric force induced by Vi develops very slowly (rate 0.1–0.5 s^{-1}) with a hyperbolic dependence of the rate on [Vi] (19). These effects have been explained with binding of Vi to the force-generating AM.ADP state after Pi release

Submitted September 27, 2010, and accepted for publication December 15, 2010.

*Correspondence: marco.linari@unifi.it

Editor: K. W. Ranatunga.

0006-3495/11/02/0665/10 $2.00

doi: 10.1016/j.bpj.2010.12.3723

(19) leading to the formation of a new AM.ADP.Vi state that dissociates from actin and accumulates as M.ADP.Vi; this second step is responsible for slow effect of Vi.

According to this scheme, 1) suppression of force by Vi can only develop during cross-bridge cycling and is proportional to the reduction in number of attached myosin motors; and 2) release of Vi and recovery of force after removal of Vi from the solution is only possible by reattachment to actin of the M.ADP.Vi state. Most investigators (20–22), however, found that addition of Vi reduces fiber stiffness less than isometric force, suggesting a Vi-induced decrease in the proportion of cross-bridge generating higher force. This conclusion is in contradiction with the view (11), supported by further experimental and modeling work from our laboratory (1,9), that force generation rapidly follows the weak-to-strong binding transition (step 3) and it is not necessary to include a further force-generating step after Pi release. More precisely, each of the biochemical states of the attached myosin motors after step 3 in Scheme 1 (AM′.ADP.Pi, AM′.ADP, and AM) is a mixture of different force-generating states in rapid equilibrium according to the strain-dependent kinetics first described in the 1971 model of Huxley and Simmons (23).

A clue for the definition of the coupling between mechanical and biochemical steps of Vi and Pi binding to the AM.ADP state of cross-bridges can be found in the analysis of the relative effects of these ligands on the ATPase rate and isometric force. Whereas increase in [Pi] reduces isometric force, but has a minor effect on the ATPase rate (2–7), increase in [Vi] reduces isometric force and ATPase rate in proportion (21). Thus, comparable mechanical effects induced by the rise in [Vi] and [Pi] imply quite different effects on the chemo-mechanical cycle.

In the work presented here, we reinvestigate the effects of Vi on the transient and steady-state mechanical characteristics of the isometric contraction and integrate these effects with the analysis of the modulation by Vi of the effects of increase in [Pi]. We estimate the number of actin-attached myosin motors from measurements of half-sarcomere stiffness, employing the recently refined methods for skinned fibers (1,10) that allows us to isolate the contributions of myosin cross-bridges and myofilaments to the half-sarcomere compliance. The results are used to further test and implement the reaction Scheme 1, identifying the different kinetic pathways related to release of Pi and binding-release of Vi at the catalytic site of the myosin motor.

MATERIALS AND METHODS

Experiments were done on glycerinated skinned fibers from psoas muscles of adult male New Zealand white rabbits (3–5 kg). Rabbits were euthanized in accordance with the European Community Council Directive 86/609/EEC. Single fiber segments (5–6-mm long) prepared as previously described (Linari et al. (10) and references therein) were attached to the lever arms of a loudspeaker motor (24) and a capacitance force transducer (sensitivity, 80–200 VN^{-1} and resonant frequency 40–50 kHz (25)) in a drop of relaxing solution. The sarcomere length (*sl*), width (*w*), and height (*h*) were measured at 0.5-mm intervals along the 3–4-mm central segment of the fiber with a 40× dry objective (NA 0.60; Carl Zeiss, Göttingen, Germany) and a 25× eyepiece. The fiber length (L_0) was set so that *sl* was 2.5 ± 0.1 μm (mean ± SD). The fiber cross-sectional area (CSA), determined assuming the fiber cross-section is elliptical, was

$$(\pi/4 \cdot w \cdot h \ =) \ 3400 \ \pm \ 800 \ \mu m^2.$$

Experimental protocol

A rapid solution exchange system allows continuous recording of length changes of a selected population of sarcomeres (500–1200) by a striation follower (26) during activation. In this system, most of force develops in the activating solution after a rapid rise of temperature from 1°C to the test temperature (1,10,27). Experiments are performed at 12°C. The following experimental protocols are used to investigate the effect of Vi.

Steady force and stiffness measurements during isometric contraction

The time course of the inhibition by Vi of steady force T_0 developed during isometric contraction of fibers activated with saturating Ca^{2+} (pCa 4.5) was determined in 10 fibers by recording a series of activation-relaxation cycles in presence of 0.1 mM Vi. For each cycle, the period of activation at the test temperature (12°C) was 3.3 s. In five fibers the time course of force inhibition by Vi was determined at different [Vi] in the range 0.1–1 mM. The change in fiber stiffness with isometric force was determined by recording the change in force elicited by step releases and stretches (rise time ~110 μs, amplitude range ±3 nm per half-sarcomere) imposed at the plateau of the isometric contraction both in control solution (0 Vi) and in presence of 0.1 mM Vi.

Development of isometric force after unloaded shortening

The time course of isometric force development at the test temperature was measured during the isometric contraction after a period of unloaded shortening (amplitude ~5% of the fiber length, duration 3 ms), either in control and in presence of 0.1 mM Vi. In four out of the 10 fibers used, the effect of Vi on force development was investigated at different values of [Pi] (range, 0–15 mM added Pi).

Data collection and analysis

Force, motor position, and sarcomere length signals were recorded with a multifunction I/O board (PCI-6110E; National Instruments, Austin, TX). A dedicated program written in LabVIEW (National Instruments) was used for signal analysis. Unless otherwise specified, data are expressed as mean ± SE.

Solutions

The composition of the solutions was determined with a program similar to that previously described (28). The starting Pi concentration was adjusted by adding KH_2PO_4 and reducing the concentration of Na_2CP and EGTA/CaEGTA to have the same ionic strength as in the control solution (no added Pi). The control solution without added Pi should contain ~1 mM Pi (29). Stock solutions of sodium orthovanadate (Na_3VO_4) (EM Science, Gibbstown, NJ) were prepared at 100 mM, pH 10.0, and boiled before use to minimize polymerization (30). After dilution of stock solution to 10 mM in rigor solution, a small aliquot of the vanadate stock solution was added directly to the relaxing, preactivating, and activating solutions to attain the desired [Vi]. Changes in the pH of the solutions were <0.1 pH units as a result of vanadate addition.

RESULTS

Effect of Vi on isometric force and stiffness of the half-sarcomere

Fig. 1 shows the time course of the effect on steady isometric force (T_0) of adding 0.1 mM Vi to the bathing solutions, as well as the time course of force recovery after removal of Vi from the solutions, for one fiber. The time of activation on the abscissa is calculated by multiplying the number of activations in solutions containing 0.1 mM Vi by the period of each activation (3.3 s). After addition of 0.1 mM Vi, T_0 declines exponentially with the time of activation to approximately half of its control value with a time constant of 13.1 s, corresponding to a rate constant of $(1/13.1\ \text{s} =) 0.076\ \text{s}^{-1}$. Taking into account the concentration of Vi used, the apparent second-order rate constant of force decay is $\sim 0.8 \times 10^3\ \text{M}^{-1}\text{s}^{-1}$. The time course of the recovery of force after Vi removal (at the time of activation = 60 s) can also be fitted by an exponential with time constant of 35.1 s, corresponding to a rate constant of $(1/35.1\ \text{s} =) 0.028\ \text{s}^{-1}$.

In four fibers, addition of 0.1 mM Vi, reduced T_0 to 0.44 ± 0.02 the control value with a rate constant of 0.09 ± 0.01 s^{-1}, corresponding to an apparent second-order rate constant of $0.9 \pm 0.1 \times 10^3\ \text{M}^{-1}\text{s}^{-1}$. This rate is slightly smaller than that reported by Dantzig and Goldman (19) ($1.34 \pm 0.30 \times 10^3\ \text{M}^{-1}\ \text{s}^{-1}$, temperature 20°C), as expected by the temperature difference. The rate constant of force recovery after removal of Vi was $3.5 \pm 1.9 \times 10^{-2}\text{s}^{-1}$, ~1/3 of that of force decay.

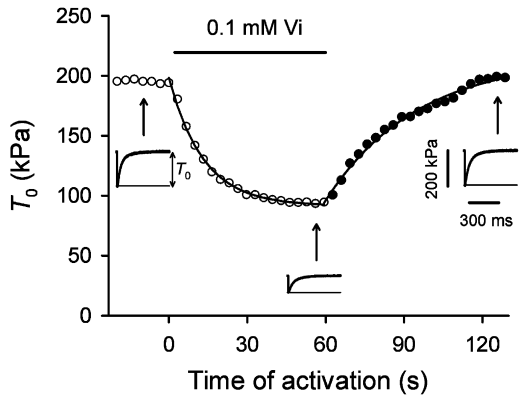

FIGURE 1 Effect of Vi on steady isometric force (T_0) after successive activations. Decay of isometric force (*open circles*) in the presence of 0.1 mM Vi (*horizontal bar*) added to the bathing solutions as function of the total time of activation at the test temperature (the duration of each activation was 3.3 s). Time zero marks the last point before addition of Vi. After 60 s of activation in presence of Vi, Vi was removed from the bathing solutions. (*Solid circles*) Recovery of isometric force as function of the total time of activation at the test temperature as before. (*Solid lines*) Exponential equations fitted to the experimental data either during force decay (from 0 to 60 s) or during force recovery (from 60 s to 130 s). The time constant was 13.1 s and 35.1 s during force decay and force rise, respectively. (*Insets*) Original records of isometric force development after the end of the unloaded shortening applied on the activated fiber at different times (as indicated by the *arrows*) before and during addition of Vi and after removal of Vi. Fiber length, 4.58 mm; sarcomere length, 2.58 μm, CSA, 4670 μm^2; temperature, 11.9°C.

Increase in [Vi] in the range 0.1–1 mM produced a progressive reduction in the final T_0 from 0.44 to 0.12 the control value (see *open circles* in Fig. 6 *B*). The decline in T_0 with time of activation becomes progressively faster with increase in [Vi]: the rate constant increases from 0.09 s^{-1} at 0.1 mM to 0.45 s^{-1} at 1 mM (see *circles* in Fig. 6 *C*). In contrast, the time course of force recovery after removal of Vi remains constant independently of [Vi] in the preceding solution (see *triangles* in Fig. 6 *C*).

The stiffness of the fiber was determined from the force responses to a series of four length steps (range −3 to +3 nm per half-sarcomere) imposed on the activated fibers both in control (Fig. 2, *A* and *C*, *a*) and in presence of 0.1 mM Vi at different steady forces and times of activation (Fig. 2, *B* and *C*, *b*). Each test step was followed by a step in opposite direction after 50 ms and the next pair of test steps in the series of four was separated from the previous pair by 200 ms. The stiffness of the half-sarcomere (k_0) was measured by the slope of the relation obtained by plotting the extreme tension attained during a length step (T_1, Huxley and Simmons (23)) versus the step amplitude per half-sarcomere (Fig. 2 *C*).

In the control solution (*circles*), the stiffness was 23.6 kPa nm^{-1} and, after the addition of 0.1 mM Vi, decreased progressively with the time of activation, but less than in proportion to T_0: k_0 was 21.1 kPa nm^{-1} at 6 s (*diamonds*) and 15.5 kPa nm^{-1} at 32 s (*triangles*). In Fig. 3 *A* (mean values from four fibers), the time courses of isometric force (*solid circles*) and stiffness (*open triangles*) after addition of Vi are shown after normalization by the control value. Stiffness decreased with an exponential time course similar to that of force, but less than force, so that when the force had attained a steady minimum value of 0.44 of the control, the stiffness had attained a steady minimum value of 0.60 of the control. The time constants of the exponential fits on the mean data points are 11.1 ± 0.6 s for the force (*continuous line*) and 16.8 ± 4.0 s for the stiffness (*dashed line*).

Analysis of the effect of Vi on the myosin cross-bridge mechanics

The abscissa intercepts of the regression lines in Fig. 2 *C*, $Y_0 (= T_0/k_0)$, provide an estimate of the strain in the elastic elements of the half-sarcomere (myofilaments and myosin cross-bridges) during the isometric contraction preceding the step (10). Y_0 decreases with the time of activation after the addition of Vi. The relation between Y_0 and T_0 measured at different times of activation is linear (*circles* in Fig. 3 *B*, mean data from four fibers) and the regression equation (*continuous line*) has a slope and an ordinate intercept of 22.3 ± 2.2 nm MPa^{-1} and 4.02 ± 0.33 nm, respectively. Both the slope and the ordinate intercept do not differ significantly ($P > 0.7$, Student's *t*-test) from the values reported in a previous study (10) as estimates of the compliance of

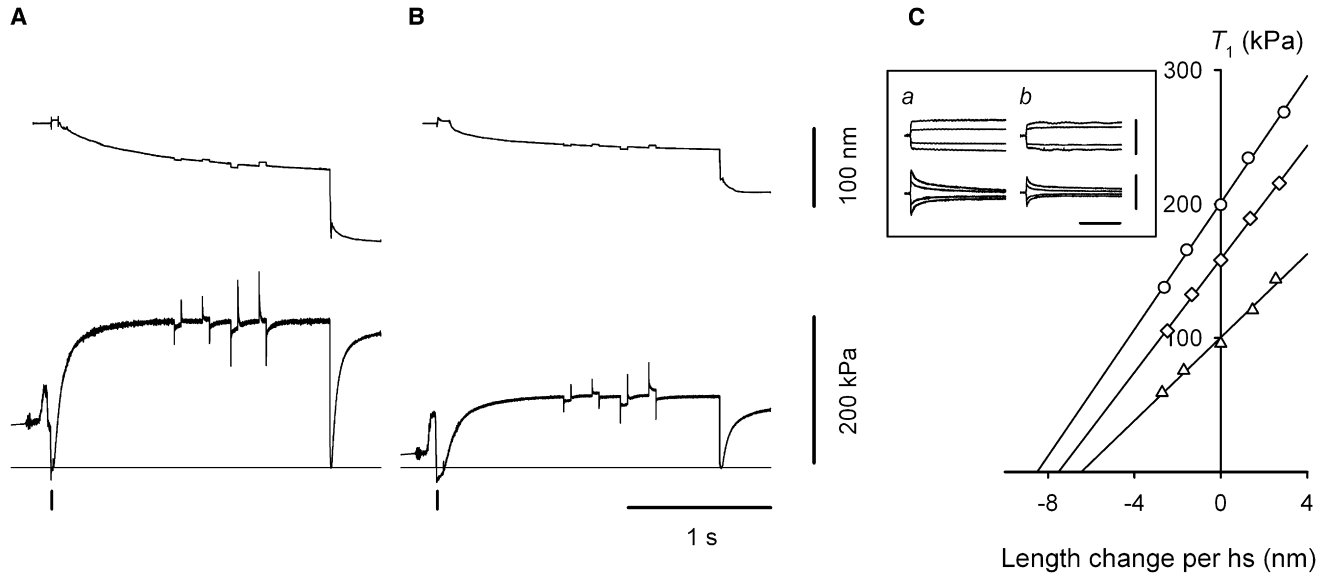

FIGURE 2 Effect of Vi on half-sarcomere stiffness. Records of sarcomere length change in nanometers per half-sarcomere (*upper traces*) and force (*lower trace*) during activation at the test temperature (starting in correspondence of the *vertical bar* next to the *horizontal line* representing zero force) in control (*A*) and after 32 s of activation after addition of Vi (*B*). During steady isometric force, a train of steps was imposed on the fiber to measure stiffness and then a large release was applied to measure zero force. (*C*) T_1 relations before (*circles*), 6 s (*diamonds*), and 32 s (*triangles*) after addition of 0.1 mM Vi. The relations are obtained by plotting the extreme force attained at the end of the step, T_1, versus the step size. Lines are linear regression equations fitted to the experimental points. (*Inset*) Superimposed force responses (*lower traces*) to step changes in half-sarcomere length (*upper traces*) in control (*a*) and in 0.1 mM Vi (*b*). Calibration bars: 10 nm per half-sarcomere, 100 kPa, and 4 ms. Fiber length, 3.86 mm; segment length under the striation follower, 0.93 mm; sarcomere length, 2.54 μm; CSA, 4020 μm^2; and temperature, 12.1°C.

the myofilaments (the slope) and the average strain of the myosin motor (the ordinate intercept) during isometric contractions at different [Ca^{2+}].

According to the analysis of the half-sarcomere compliance (31,32), the half-sarcomere strain is given by the sum of the strain of myofilaments, $C_f^* T_0$, and the strain of myosin cross-bridges acting in parallel in the half-sarcomere, $s = T_0/(\beta^* e_0)$, where $\beta^* e_0$ is the stiffness of the cross-bridges, given by the product of the stiffness of the array of myosin heads if all heads are attached to actin (e_0) and the fraction of myosin heads that are attached (β).

Triangles in Fig. 3 *B* are the values of *s* obtained after subtracting from the half-sarcomere strain (*circles*) the contribution of the myofilament compliance (estimated by the slope of the regression line fitted to *circles*). It is evident that the reduction of T_0 by Vi does not imply any systematic change in *s* (the *dashed line* is the linear fit to *triangles*), and therefore in the force generated by the myosin motors. Consequently the stiffness of the array of cross-bridges working in parallel in the half-sarcomere, e_0, estimated by the ratio T_0/s, decreases in proportion to T_0 at various times after addition of Vi (*open circles* in Fig. 3 *A*), indicating that

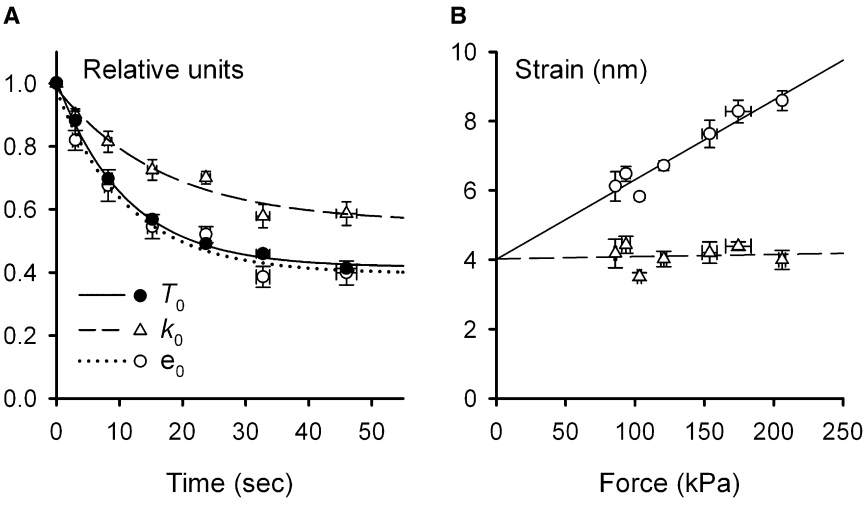

FIGURE 3 Effect of Vi on the mechanical parameters of the half-sarcomere and of the myosin cross-bridges. (*A*) Decay of isometric force (T_0, *solid circles*), stiffness of the half-sarcomere (k_0, *triangles*), and stiffness of array of cross-bridges in the half-sarcomere (e_0, *open circles*) during activation of the fiber after addition of 0.1 mM Vi. Lines are exponential fits to T_0 (*continuous line*), k_0 (*dashed line*), and e_0 (*dotted line*). The time constant of the fits are 11.1 ± 0.6 s for T_0, 16.8 ± 4.0 s for k_0, and 11.3 ± 1.9 s for e_0. (*B*) Strain in the half-sarcomere (Y_0, *circles*) and of the myosin cross-bridges (s_0, *triangles*) plotted against the isometric force at various times after addition of Vi. (*Solid line*) Linear regression fitted to the circles (ordinate intercept, 4.02 ± 0.33 nm; slope, 22.3 ± 2.2 nm MPa^{-1}). (*Dashed line*) Linear regression fitted to the triangles (ordinate intercept, 4.02 ± 0.33 nm; slope, 0.04 ± 2.2 nm MPa^{-1}). Values are mean ± SE from four fibers.

the reduction of T_0 is fully accounted for by the reduction in number of attached myosin motors. The time constant of the exponential fit on the mean data points to e_0 (*dotted line*) is 11.3 ± 1.9 s.

Effect of Vi on the relation between isometric force and [Pi]

The effect of 0.1 mM Vi on isometric force was investigated in four fibers for a range of added Pi concentrations between 0 and 15 mM. Isometric force (T_0) was first determined at different [Pi] in control, then 0.1 mM Vi was added and, after isometric force was reduced to a steady value, Pi-dependence of isometric force was determined again. As shown in Fig. 4, the inhibitory effect of the increase in [Pi] is maintained in presence of 0.1 mM Vi (*solid diamonds*) as in the control (*open circles*), even though the addition of Vi per se has already decreased the isometric force without added Pi to 0.42 the control.

Once the isometric force at each [Pi] is normalized by the respective value without added Pi, the relation between force and [Pi] in presence of 0.1 mM Vi (*solid circles*) superposes on that without Vi. This result shows that, in the presence of Vi, a given concentration of Pi reduces the force proportionally to the fraction of force-producing cross-bridges remaining after the reduction caused by Vi. Thus, Pi acts on a population of force-generating myosin motors that has survived the action of Vi, indicating two different pathways for the reduction of force generating myosin motors.

Effect of Vi on the rate of isometric force development

The time course of isometric force development was measured during the isometric contraction after the end of a period of unloaded shortening as reported in Caremani et al. (1). As shown in Fig. 5, *A* (force in kPa) and *B* (force relative to the isometric force before the unloaded shortening), without added Pi the force development (T_r) has a quite similar time course either in control (*shaded trace*) or in 0.1 mM Vi (*solid trace*). T_r then can be fitted by means of a biexponential equation, $T_r = T_F(1 - \exp(-r_F t)) + T_S(1 - \exp(-r_S t))$, where t is the time elapsed from the start of force development after the end of shortening, T_F and T_S are the amplitudes, and r_F and r_S are the rate constants of the fast and the slow exponentials, respectively. In agreement with previous work (1), T_F and T_S are ~0.7 and ~0.3, respectively, independently of the presence of Vi, and r_F and r_S are ~24 s^{-1} and ~6 s^{-1}, respectively, and again not significantly affected by addition of Vi (see Table S1 in the Supporting Material). The absence of Vi effect on these parameters has been previously found also in skinned trabeculae from rat heart (22).

Fig. 5 *C* shows the dependencies on [Pi] of r_F (*circles*) and r_S (*triangles*) either in control (*open symbols*) or in 0.1 mM Vi (*solid symbols*). The rate constant of the fast component r_F increases with [Pi] with a slope that progressively reduces (1). The r_F−[Pi] relation remains identical after the addition of Vi.

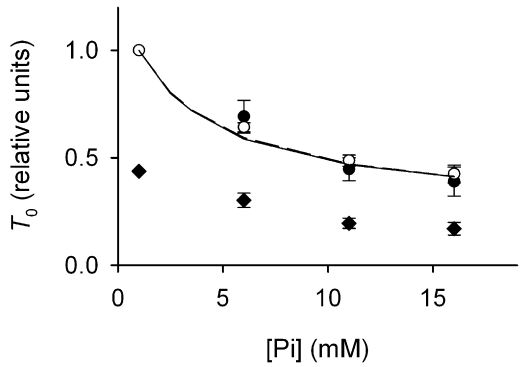

FIGURE 4 Effect of Vi on Pi-dependence of isometric force (T_0) in control (*open circles*) and in 0.1 mM Vi (*solid circles* and *diamonds*). Note that diamonds are relative to the T_0 in control and without added Pi, and solid circles are relative to T_0 in 0.1 mM Vi without added Pi. Values are mean ± SE from four fibers. Lines are the responses of the simulation in control (*continuous line*) and in presence of 0.1 mM Vi (*dashed line*).

MODEL SIMULATION

The constraints that drive the kinetic model, originated from this and previous work (9), are:

1. The suppression of isometric force by Vi is accompanied by a proportional reduction in both the number of actin attached myosin motors (Fig. 3 *A*) and the ATPase rate (21).
2. The rate constant of suppression of isometric force by Vi is quite low (<0.1 s^{-1} at 0.1 mM Vi) and increases with the concentration of Vi attaining a maximum of 0.45 s^{-1} at 1 mM Vi (19). The rate constant of force recovery after removal of Vi is independent of [Vi] (triangles in Fig. 6 C).
3. The mechanism of the reduction in force induced by Vi is similar to that induced by Pi, as it is explained by a proportional drop in number of attached myosin motors without any effect on the force per motor (compare triangles in Fig. 3 B of this work and in Fig. 1 D of Caremani et al. (1)). However, the underlying biochemical pathway is different, as, in contrast to the effect of Vi reported at point 1, the increase of [Pi] has a much smaller effect on the ATPase rate (5–7).
4. In further contrast with the effect of Pi, increase in [Vi] does not increase the rate of isometric force development (Fig. 5).
5. Pi acts on the fraction of cross-bridges survived to Vi action (Fig. 4), indicating that cross-bridges in the AM.ADP state are in equilibrium with both an AM.ADP.Pi state and an AM.ADP.Vi state: whereas the first complex allows cross-bridge detachment and completion of the ATP hydrolysis cycle through product

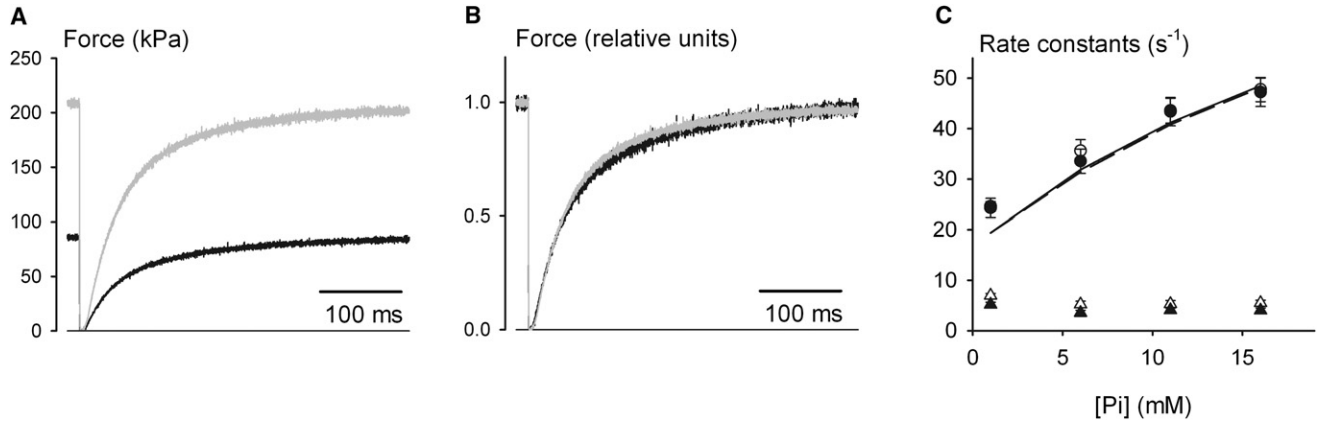

FIGURE 5 Effect of Vi on Pi-dependence of the rate of isometric force development. (*A*) Force development in control (*shading*) and in 0.1 mM Vi (*solid*). (*B*) Same traces as in panel *A* after normalization for the final steady force value. Fiber length, 3.97 mm; sarcomere length, 2.40 μm; CSA, 4340 μm^2; temperature, 11.9°C. (*C*) Pi-dependence of the rate constants of the fast (r_F, *circles*) and of the slow (r_S, *triangles*) exponential components in control (*open symbols*) and in 0.1 mM Vi (*solid symbols*). Values are mean ± SE from four fibers. (*Lines*) Responses of the simulation in control (*continuous line*) and in presence of 0.1 mM Vi (*dashed line*).

release (9), the second complex allows cross-bridge detachment with accumulation in a M.ADP.Vi state that is not able to complete the ATPase cycle and can reenter the cycle only via reattachment to actin, once Vi is removed from the solution (19).

Scheme 1 of the myosin-actin ATPase cycle described in the Introduction must be integrated according to Scheme 2, as follows:

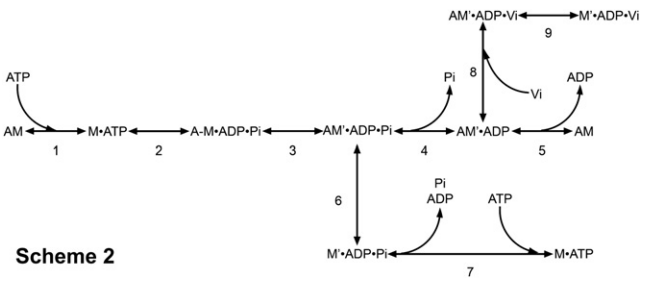

Scheme 2

The scheme takes into account the conclusion from previous work with radioactively labeled Vi and nucleotides (19) that AM′.ADP is the sole intermediate state to which Vi can readily bind (step 8). This is followed by a slower detachment from actin with the formation of a stable M′.ADP.Vi complex (step 9). In agreement with the evidence from Dantzig and Goldman (19), the only way to release the bound Vi, once Vi has been removed from the solution, is via reattachment to actin of the myosin heads in the M′.ADP.Vi state. For simplicity we assume here that the AM′.ADP.Vi state of the cross-bridges is a force-producing state, just like the other strongly bound states AM′.ADP.Pi, AM′.ADP, and AM (but see later for further consideration on this point).

The set of rate constants reported in Table S2, used for the simulation of mechanical and energetic responses reported in Fig. 6, has been obtained by adding the rate constants of the additional path (steps 8 and 9), selected to fit the effects of Vi, to the set of rate constants selected by Linari et al. (9) (Scheme 2).

Simulation of the effect of Vi on isometric force

In Fig. 6 *A* are shown the results of the simulation (*solid symbols*) for the time courses of the decrease of steady isometric force induced by addition of Vi at three different concentrations (0.05 mM, *triangles*; 0.1 mM, *circles*; and 1 mM, *diamonds*) and the subsequent recovery after removal of Vi (*open symbols*). It can be seen that, at higher [Vi], the force suppression is larger and faster, while the rate of force recovery is independent of [Vi].

The results of the simulation in the range of Vi concentrations up to 1 mM Vi are summarized in Fig. 6 *B* (*continuous line*) for the Vi dependence of the amplitude of the force suppression, and in Fig. 6 *C* for the Vi dependence of the rate constant of force suppression (*continuous line*) and the rate constant of force recovery after removal of Vi (*dashed line*). It can be seen that the model is able to satisfactorily reproduce the observed Vi dependence of all mechanical parameters (*symbols* in Fig. 6, *B* and *C*).

According to the model, the dependence on Vi of the observed rate constant of force suppression (*circles* in Fig. 6 *C*) is related to the kinetic assumption (19) that V_i binding to AM′.ADP state (step 8) is relatively fast with respect to the following detachment from actin (step 9). Under these conditions, the rate constant of force suppression ranges from 3.5×10^{-2} s^{-1} ($= k_{-9}$), for [Vi] approaching zero, to 1.5 s^{-1} ($= k_9 + k_{-9}$) for [Vi] approaching ∞. The slope of the relation depends on K_8, that is set to ~1×10^3 M^{-1} to fit the changes in the rate constant of force suppression (*continuous line* in Fig. 6 *C*). The same kinetic scheme predicts that the rate constant of force recovery after

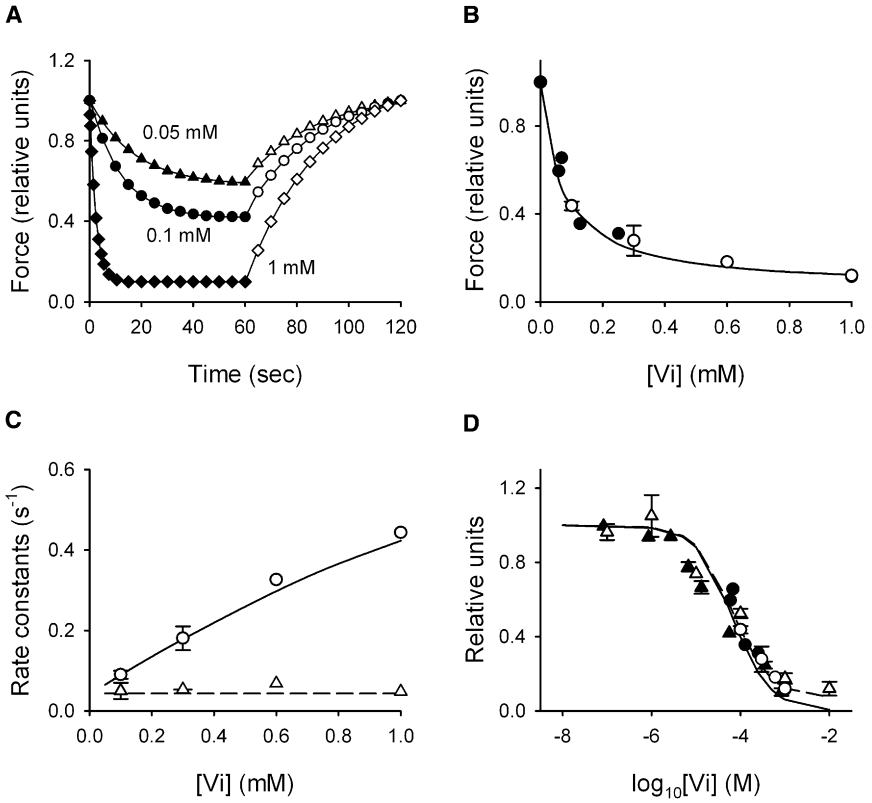

FIGURE 6 Responses of the simulation with the kinetic Scheme 2. (*A*) Simulated time course of suppression (*solid symbols*) and recovery (*open symbols*) of isometric force for three different [Vi] (0.05 mM, 0.1 mM, and 1 mM), as indicated by the figures close to the traces. Lines are single exponential equations fitted to the points during force suppression (from 0 to 60 s) and during force recovery (from 60 s to 120 s). (*B*) Dependence on [Vi] of isometric force when the force suppression has attained a steady value. *Solid circles* from Fig. 3 *A* of Dantzig and Goldman (19); *open circles* our values with 0.1, 0.3 (three fibers), 0.6 (one fiber), and 1 mM Vi (one fiber). *Continuous line*, model simulation. (*C*) Dependence on [Vi] of rate of force suppression (*circles*, data; and *continuous line*, model) and recovery (*triangles*, data; and *dashed line*, model). Symbols are for the same Vi experiments as open circles in panel *B*. (*D*) Dependence on [Vi] of isometric force (*solid* and *open circles* as in *B*, and *solid triangles* from Fig. 2 of Wilson et al. (21)) and ATPase rate (*open triangles* from Fig. 6 of Wilson et al. (21)). *Continuous line* response of the model for the ATPase rate and isometric force if the AM′.ADP.Vi state of cross-bridges does not bear force. *Dashed line* response of the model for the isometric force if the AM′.ADP.Vi state bears force.

the removal of Vi is 3.5×10^{-2} s^{-1} ($= k_{-9}$) and is independent of [Vi] (compare *triangles* and *dashed line* in Fig. 6 *C*).

Simulation of the effect of Vi on isometric ATPase rate

The predictions of the model as regards the effect of [Vi] on the ATPase rate are reported in Fig. 6 *D* (*continuous line*). The plot is in log[Vi] scale and the abscissa values range from −8 to −2 to be comparable to the observed ATPase rate (*open triangles*) and isometric force (*solid triangles*) reported from Wilson et al. (21). The dashed line is the force-log[Vi] relation predicted by the model. Circles are the force data from Fig. 6 *B* (*open circles,* this work; *solid circles*, from Dantzig and Goldman (19)). It can be seen that, notwithstanding the different [Pi] and temperature in the experiments of Wilson et al. (21) (5 mM and 25°C, respectively), the observed data from different sources almost superpose each other and with the predictions of the model.

For [Vi] > 1 mM, the simulated force (*dashed line*) remains slightly higher with respect to the simulated ATPase rate (*continuous line*). This is the consequence of the assumption that the cross-bridges in the AM′.ADP.Vi state are force-generating. In fact, by subtracting the contribution of this state from isometric force, the simulated force-log[Vi] relation coincides with that of the ATPase rate. In any case, comparison of simulations with data in Fig. 6 *D* makes it evident that no conclusion can be drawn on whether or not AM′.ADP.Vi is a force-generating state, because 1) at [Vi] < 1 mM, the occupancy of the AM′.ADP.Vi state is so small that there is not substantial difference in the effect of Vi on isometric force and ATPase rate, and 2) at [Vi] > 1 mM, there cannot be an adequate experimental evidence for solving the question. In fact, as reported by Dantzig and Goldman (19) and references therein, experiments at high [Vi] become unreliable for the tendency of Vi to polymerize or to be reduced to VO^{2+} by glutathione.

Simulation of the effect of Vi on Pi-modulated mechanical responses

The predictions of the model of the effects of [Vi] on the relation between isometric force and [Pi] are compared to the observed relation in Fig. 4. It can be seen that, in agreement with the experimental results, the drop in force (and in number of attached motors) with increase in [Pi], relative to the value without added Pi, is identical in absence of Vi (*continuous line*, model; *open circles*, data) and in presence of 0.1 mM Vi (*dashed line*, model; *solid circles*, data). Thus the effect of increasing [Pi] is the same in control as in the presence of 0.1 mM Vi, but in this last case, ~55% of myosin motors have been sequestered in the M′.ADP.Vi state and Pi acts only on the remaining 45%. This mechanism is confirmed by the identity of the relations of the rate constant

of force development and [Pi] (Fig. 5 *C*) both in control (*continuous line*, model; *open circles*, data) and in solution with 0.1 mM Vi (*dashed line*, model; *solid circles*, data).

The absence of effect of [Vi] on the dependence on [Pi] of the kinetics of the transient and steady-state mechanical responses is the consequence of the 10-times-slower kinetics of detachment/attachment from/to actin promoted by Vi (step 9), with respect to that promoted by Pi (steps 3 and 6). At the same time, it must be noted that the apparent second-order rate constant of Vi binding (~1×10^3 M^{-1} s^{-1}; see Dantzig and Goldman (19) and this work) is comparable to that of Pi binding to the same state (5×10^3 M^{-1} s^{-1}; see Hibberd et al. (33)).

DISCUSSION

The effects of Vi on mechanics and energetics of force generation by muscle myosin

The addition of Vi to the solution decreases the force generated by the array of myosin motors acting in parallel in the half-sarcomere by the binding of Vi to the force-generating AM′.ADP state of the cross-bridges and subsequent detachment with accumulation in a M′.ADP.Vi state. The effect implies a proportional reduction in the number of actin attached myosin motors and in the ATPase rate.

Even though Vi and Pi bind to the same AM′.ADP state during isometric contraction, they exert a quite different action in the catalytic site of the myosin head. In an environment with increased Pi, the Pi mass action promotes detachment of the strongly bound force-generating AM′.ADP.Pi myosin heads from actin, either by reversing the weak to strong binding transition (step 3 in Linari et al. (9); see also Geeves and Holmes (34)), or by populating a M′.ADP.Pi state that rapidly releases the hydrolysis products (steps 6 and 7 in Linari et al. (9)). This second path implies that the myosin cross-bridge during isometric force generation has irreversibly gone through the liberation of part of the free energy of ATP hydrolysis and therefore, after detachment, is committed for completing the biochemical cycle and rebinding a new ATP. In this way, a high isometric ATPase rate is maintained even at high [Pi] (2–7), when the number of attached myosin motors is reduced (8).

Binding of Vi to the strong bound force-generating AM′.ADP state opens a new possibility of detachment from actin that provides accumulation in a M′.ADP.Vi state, and thus, subtraction of myosin motors from the force-producing ATPase cycle.

These conclusions are in contradiction with the view of Cooke and collaborators, suggested by the steep relation between isometric force and log [Vi] (~2 log [Vi] units for 100% force suppression; see Fig. 8 in Wilson et al. (21)), that the AM.ADP state of cross-bridges to which Vi binds is a nonforce-generating state weakly bound to actin and therefore characterized by a narrow range of free energy values (<4 k_BT, where k_B is the Boltzmann constant and T is absolute temperature).

Alternatively, the AM.ADP state could be a force-generating state, but still characterized by a narrow range of free energy values, if all cross-bridges during isometric contraction were distributed toward the beginning of the working stroke. This possibility, which was mentioned by Cooke and collaborators, appears now as the most likely solution to the problem, after the demonstration that the stiffness of the myosin motor is too high for the generation of isometric force to be thermodynamically compatible with the 11-nm working stroke indicated by the crystallographic model (34). In fact, the structural change responsible for isometric force has been found not larger than 2–3 nm (10,35,36), and under these conditions the free energy change associated to force generation is smaller than 4 k_BT (9), in agreement with the range of free energy values attributed to the AM.ADP state to fit the observed relation between isometric force and log[Vi] (21).

The recovery of isometric force after removal of Vi from the solution occurs via rebinding of the M′.ADP.Vi state to actin, which allows the myosin motor to reenter the ATP hydrolysis cycle. All these effects are consistent with the scheme of reactions suggested by Dantzig and Goldman (19), that here is explicitly reported as Scheme 2.

Using Scheme 2, we are able to reproduce all the relevant mechanical and energetic data reported in the section on Model Simulation (above):

1. The Vi dependence of the amplitude and rate of isometric force suppression and recovery (Fig. 6, *A–C*).
2. The similarity of the relation between decrease of isometric force (and number of attached myosin motors) and decrease of the ATPase rate (Fig. 6 *D*).
3. The identity of the relation between isometric force and [Pi] in absence and in presence of 0.1 mM Vi that reduces the isometric force in absence of Pi to ~0.4 the control (Fig. 4).
4. The absence of any effect of Vi on the rate constant of isometric force development and on the relation between rate of force development and [Pi] (Fig. 5 *C*).

Effects of Vi and Pi in terms of the crystallographic model of the working stroke

The finding that the increase of [Pi] reduces the isometric ATPase rate much less than the number of force-generating myosin motors cannot be explained by the idea that, under high load, the presence of Pi in the nucleotide-binding pocket keeps low the probability for the actin-binding cleft to irreversibly evolve toward the formation of a strong interaction with actin (34). In fact, in this case, the ATPase would be inhibited by increase in [Pi] in the same way as the formation of the strong binding interface with actin.

Another unconventional path, hypothesized to solve the discrepancy between the number of active myosin motors and the ATPase rate at high [Pi], consists in the possibility that detachment from actin occurs also directly from the strongly bound force-generating AM′.ADP.Pi state and therefore after the occurrence of an irreversible structural change in the nucleotide-binding pocket.

The increase in the apparent rate constant for detachment through both steps 3 and 6 explains the Pi-dependent increase in the rate of development of isometric force. The generation of a detached M′.ADP.Pi state from an attached force-generating myosin head, that has undergone an irreversible structural change, implies the removal of the mechanical constraints that prevent the completion of the working stroke, so that these myosin heads rapidly proceed through the sequence of events including lever-arm tilting toward the end of the working stroke and opening of the nucleotide-binding pocket with release of the hydrolysis products. The Pi promoted increase of the flux through this path explains the maintenance of a high ATPase rate.

Substitution of Pi with Vi in the complex with the strongly bound force-generating AM′.ADP state reproduces only partially the effects of increased Pi. The reduction of isometric force and of the number of force-generating motors is not accompanied by an increase in the rate constant of isometric force generation, indicating that the apparent rate constant for detachment through steps 3 and 6 is not increased. A further fundamental difference is that the AM′.ADP.Vi complex slowly detaches from actin to populate a M′.ADP.Vi state that cannot release Vi and ADP to start a new ATPase cycle.

Presumably, when Vi is present in the nucleotide-binding pocket in place of Pi, detachment from actin generates a myosin head that maintains both the lever arm in the prepower stroke conformation and the nucleotide-binding pocket in the closed conformation, as expected from the crystallographic structure (34,37). This explains why Vi is not released from the catalytic site after its removal from the solution. The only way for the Vi to be released and the cross-bridge to complete the cycle is via the reattachment of the M′ADP.Vi complex to actin.

SUPPORTING MATERIAL

Two tables are available at http://www.biophysj.org/biophysj/supplemental/S0006-3495(10)05296-3.

The authors thank Mario Dolfi for skilled technical assistance. This research was supported by the Ministero della Salute (Italy), grant No. MUL-2007-666195, and by the Ente Cassa di Risparmio di Firenze (Italy), grant No. 2009-1179.

REFERENCES

1. Caremani, M., J. Dantzig, …, M. Linari. 2008. Effect of inorganic phosphate on the force and number of myosin cross-bridges during the isometric contraction of permeabilized muscle fibers from rabbit psoas. *Biophys. J.* 95:5798–5808.
2. Kawai, M., K. Güth, …, J. C. Rüegg. 1987. The effect of inorganic phosphate on the ATP hydrolysis rate and the tension transients in chemically skinned rabbit psoas fibers. *Pflugers Arch.* 408:1–9.
3. Cooke, R., K. Franks, …, E. Pate. 1988. The inhibition of rabbit skeletal muscle contraction by hydrogen ions and phosphate. *J. Physiol.* 395:77–97.
4. Webb, M. R., M. G. Hibberd, …, D. R. Trentham. 1986. Oxygen exchange between Pi in the medium and water during ATP hydrolysis mediated by skinned fibers from rabbit skeletal muscle. Evidence for Pi binding to a force-generating state. *J. Biol. Chem.* 261:15557–15564.
5. Bowater, R., and J. Sleep. 1988. Demembranated muscle fibers catalyze a more rapid exchange between phosphate and adenosine triphosphate than actomyosin subfragment 1. *Biochemistry.* 27:5314–5323.
6. Postma, E. J., I. A. van Graas, and G. J. Stienen. 1995. Influence of inorganic phosphate and pH on ATP utilization in fast and slow skeletal muscle fibers. *Biophys. J.* 69:2580–2589.
7. Potma, E. J., and G. J. Stienen. 1996. Increase in ATP consumption during shortening in skinned fibers from rabbit psoas muscle: effects of inorganic phosphate. *J. Physiol.* 496:1–12.
8. Pate, E., and R. Cooke. 1989. A model of crossbridge action: the effects of ATP, ADP and Pi. *J. Muscle Res. Cell Motil.* 10:181–196.
9. Linari, M., M. Caremani, and V. Lombardi. 2010. A kinetic model that explains the effect of inorganic phosphate on the mechanics and energetics of isometric contraction of fast skeletal muscle. *Proc. Biol. Sci.* 277:19–27.
10. Linari, M., M. Caremani, …, V. Lombardi. 2007. Stiffness and fraction of myosin motors responsible for active force in permeabilized muscle fibers from rabbit psoas. *Biophys. J.* 92:2476–2490.
11. Dantzig, J. A., Y. E. Goldman, …, E. Homsher. 1992. Reversal of the cross-bridge force-generating transition by photogeneration of phosphate in rabbit psoas muscle fibers. *J. Physiol.* 451:247–278.
12. Nyitrai, M., and M. A. Geeves. 2004. Adenosine diphosphate and strain sensitivity in myosin motors. *Philos. Trans. R. Soc. Lond. B Biol. Sci.* 359:1867–1877.
13. Sleep, J., M. Irving, and K. Burton. 2005. The ATP hydrolysis and phosphate release steps control the time course of force development in rabbit skeletal muscle. *J. Physiol.* 563:671–687.
14. West, T. G., M. A. Ferenczi, …, N. A. Curtin. 2005. Influence of ionic strength on the time course of force development and phosphate release by dogfish muscle fibers. *J. Physiol.* 567:989–1000.
15. Goodno, C. C. 1979. Inhibition of myosin ATPase by vanadate ion. *Proc. Natl. Acad. Sci. USA.* 76:2620–2624.
16. Goodno, C. C., and E. W. Taylor. 1982. Inhibition of actomyosin ATPase by vanadate. *Proc. Natl. Acad. Sci. USA.* 79:21–25.
17. Goody, R. S., W. Hofmann, …, C. C. Goodno. 1980. Relaxation of glycerinated insect flight muscle by vanadate. *J. Muscle Res. Cell Motil.* 1:198–199.
18. Magid, A., and C. C. Goodno. 1982. Inhibition of cross-bridge force by vanadate ion. *Biophys. J.* 37:107a.
19. Dantzig, J. A., and Y. E. Goldman. 1985. Suppression of muscle contraction by vanadate. Mechanical and ligand binding studies on glycerol-extracted rabbit fibers. *J. Gen. Physiol.* 86:305–327.
20. Chase, P. B., D. A. Martyn, …, A. M. Gordon. 1993. Effects of inorganic phosphate analogues on stiffness and unloaded shortening of skinned muscle fibers from rabbit. *J. Physiol.* 460:231–246.
21. Wilson, G. J., S. E. Shull, and R. Cooke. 1995. Inhibition of muscle force by vanadate. *Biophys. J.* 68:216–226.
22. Martyn, D. A., L. Smith, …, M. Regnier. 2007. The effects of force inhibition by sodium vanadate on cross-bridge binding, force redevelopment, and Ca^{2+} activation in cardiac muscle. *Biophys. J.* 92:4379–4390.
23. Huxley, A. F., and R. M. Simmons. 1971. Proposed mechanism of force generation in striated muscle. *Nature.* 233:533–538.

24. Lombardi, V., and G. Piazzesi. 1990. The contractile response during steady lengthening of stimulated frog muscle fibers. *J. Physiol.* 431:141–171.

25. Huxley, A. F., and V. Lombardi. 1980. A sensitive force transducer with resonant frequency 50 kHz. *J. Physiol.* 305:15–16.

26. Huxley, A. F., V. Lombardi, and L. D. Peachey. 1981. A system for fast recording of longitudinal displacement of a striated muscle fiber. *J. Physiol.* 317:12P–13P.

27. Linari, M., R. Bottinelli, …, V. Lombardi. 2004. The mechanism of the force response to stretch in human skinned muscle fibers with different myosin isoforms. *J. Physiol.* 554:335–352.

28. Brandt, P. W., J. P. Reuben, and H. Grundfest. 1972. Regulation of tension in the skinned crayfish muscle fiber. II. Role of calcium. *J. Gen. Physiol.* 59:305–317.

29. Pate, E., and R. Cooke. 1989. Addition of phosphate to active muscle fibers probes actomyosin states within the powerstroke. *Pflugers Arch.* 414:73–81.

30. Goodno, C. C. 1982. Myosin active-site trapping with vanadate ion. *Meth. Enzymol.* 85:116–123.

31. Ford, L. E., A. F. Huxley, and R. M. Simmons. 1981. The relation between stiffness and filament overlap in stimulated frog muscle fibers. *J. Physiol.* 311:219–249.

32. Linari, M., I. Dobbie, …, V. Lombardi. 1998. The stiffness of skeletal muscle in isometric contraction and rigor: the fraction of myosin heads bound to actin. *Biophys. J.* 74:2459–2473.

33. Hibberd, M. G., J. A. Dantzig, …, Y. E. Goldman. 1985. Phosphate release and force generation in skeletal muscle fibers. *Science.* 228:1317–1319.

34. Geeves, M. A., and K. C. Holmes. 2005. The molecular mechanism of muscle contraction. *Adv. Protein Chem.* 71:161–193.

35. Decostre, V., P. Bianco, …, G. Piazzesi. 2005. Effect of temperature on the working stroke of muscle myosin. *Proc. Natl. Acad. Sci. USA.* 102:13927–13932.

36. Piazzesi, G., M. Reconditi, …, V. Lombardi. 2007. Skeletal muscle performance determined by modulation of number of myosin motors rather than motor force or stroke size. *Cell.* 131:784–795.

37. Smith, C. A., and I. Rayment. 1996. X-ray structure of the magnesium (II).ADP.vanadate complex of the *Dictyostelium discoideum* myosin motor domain to 1.9 Å resolution. *Biochemistry.* 35:5404–5417.